Computational Fluid Dynamics Laboratory 2

Group 5: Akshat Pratap Singh (22110023), Astitva Aryan (22110041), Hari Balaji (22110092), Nikhil Kumar (22110166), Nimesh Goyal (22110168)

Department of Mechanical Engineering, IIT Gandhinagar

Under Prof. Dilip Srinivas Sundaram and Prof. Uddipta Ghosh

***Abstract*—*This report includes the answers to the questions presented in the CFD Lab 2 for the ME 207 course. It attempts to use the ANSYS simulation software to simulate the laminar pipe flow problem and interpret the simulation results effectively. The findings after the simulation contribute to a better understanding of airfoil aerodynamics, enabling the optimizations for improved performance in various applications.*

***Keywords*—*CFD, ANSYS, NACA 0012, Airfoil, Aerodynamics, Laminar Flow, Mesh Independence, Drag Coefficient, Lift Coefficient*

1. Introduction

Airfoil design and analysis play a crucial role in the aerodynamic performance of aircraft and turbomachinery components. Computational Fluid Dynamics (CFD) simulations provide a powerful tool for studying the flow behavior around airfoils, enabling engineers to predict aerodynamic forces, flow patterns, and potential flow separation under various flow conditions.

In this study, we focus on the laminar flow over a NACA 0012 airfoil section with a chord length of 1 meter. The primary objectives of this project are to create a 2D computational domain around the NACA 0012 airfoil, apply appropriate boundary conditions, and investigate the aerodynamic performance at angles of attack of 0° and 5°. By calculating the drag and lift coefficients and analyzing the velocity, pressure, and streamline contours, we aim to gain insights into the flow behavior, boundary layer development, and potential flow separation phenomena. Additionally, a mesh independence study will be conducted to ensure the accuracy and reliability of the simulation results.

The findings from this CFD analysis will contribute to a better understanding of airfoil aerodynamics, enabling the optimization of airfoil designs for improved lift-to-drag ratios and overall performance in various applications, including aircraft wings and turbomachinery blades.

2. Geometry and Boundary Conditions

Given Data:
$U_\infty = 30$ m/s, $T_{air} = 25°C$, $\rho_{air} = 1.225$ kg/m^3, $\nu_{air} = 1.81 \times 10^{-5}$ Pa s

- **Geometry:** For analyzing the given cylindrical pipe, an airfoil of the given dimensions was utilised, and a computational domain around it was defined to determine the fluid flow behaviour around the airfoil.
- **Boundary Conditions:**
  Inlet: The inlet boundary condition is the inlet velocity, which is determined using the Reynolds Number.
  Outlet: The outlet boundary condition is the specification of the pressure at the Outlet.
  Airfoil Surface: The no-slip boundary condition is applied at the surface of the airfoil to account for viscous effects.

3. Mesh Statistics and Mesh Independence Study

This simulation's mesh was created differently than the previous CFD simulation. Owing to the airfoil's shape, the computational domain around the airfoil was divided into six parts, so meshing becomes easier.
Here is the completed and fully meshed computational domain visualized:

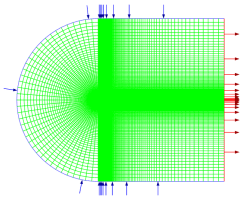

Figure 1. *Visualised Computational Domain*

3.1. Mesh Statistics

Below are the relevant statistics of the primary mesh used to perform the simulation:

Physics Preference	CFD
Solver Preference	Fluent
Nodes	34340
Elements	34000

Table 1. *Mesh Statistics*

3.2. Mesh Independence Study

To demonstrate mesh independence, there should be a very small or negligible difference in the values on convergence. The values obtained are as follows:

Refinement Level	Number of Nodes	Number of Elements
Level 1	19456	19200
Level 2	34340	34000
Level 3	77010	76500

Table 2. *Nodes and Elements in the Three Levels of Mesh Refinement*

Refinement Level	Convergence Iteration	Drag Coefficient	Lift Coefficient
Level 1	162	0.0084	0.0001
Level 2	169	0.007	0.00
Level 3	180	0.0055	0.00

Table 3. *Values for Different Levels of Mesh Refinement*

The parameters chosen to demonstrate the independence of mesh refinement were the coefficients of lift and drag, c_d and c_l, respectively. This was because these were the values we needed to calculate, and they provide an excellent measure to determine if the simulation is mesh-independent.

From table 3, we can see that the variation in the values of c_d and c_l is minimal between multiple iterations of mesh refinement, and it decreases as we refine the mesh further. We can hence say that the results are mesh-independent.

4. Discretisation Schemes and Solution Methodology

4.1. Discretisation Schemes

The software used to perform this laboratory was ANSYS. The discretization schemes used were:

1. **Finite Volume Method (FVM):** This is the core discretization scheme used in ANSYS's Fluent Solver for CFD. Fluent discretizes the computational domain into a mesh of control volumes, calculates the fluxes across the faces of these control volumes, and integrates the governing equations over each control volume to obtain numerical solutions.

2. **Spatial Discretisation Schemes:** Some spatial discretization schemes, like first and second-order upwind schemes, quick schemes, etc., may have been used by the solver. Besides these, the Fluent solver uses temporal discretization schemes, turbulence modeling schemes, and scalar transport schemes.

4.2. Solution Methodology

[1] ANSYS's Fluent Solver uses the above discretization schemes to obtain the solutions for the continuity, x-velocity, and y-velocity.
The process followed to obtain the solution was streamlined by ANSYS as follows:

1. **Geometry:** Used to define the geometry of the domain to be analyzed. This was done by using Airfoil Tools' NACA 4-digit airfoil generator[2]. The text file obtained was formatted using Microsoft Excel and then loaded into ANSYS. The computational domain was also drawn as a sketch, and it was divided into six sections for convenient meshing.

2. **Mesh:** Used to define the mesh, enabling the discretization of the geometrical domain. The six sections defined in the geometry were meshed accordingly so that there were no discrepancies in the meshing.

3. **Setup:** Used to define boundary conditions and other parameters before computing the solution.
   - Scheme for Pressure-Velocity Coupling: *Coupling*
   - Flux Type for Pressure-Velocity Coupling: *Rhie-Chow (momentum based)*
   - Gradient for Spatial Discretization: *Least Square Cell Based*
   - Pressure for Spatial Discretization: *Second Order*
   - Momentum for Spatial Discretization: *Second Order Upwind*
   - Psuedo Time Method: *Global Time Step*

4. **Solution:** Computing the solution after defining all the required parameters. We utilised hybrid initialisation, and the maximum number of iterations was set to 1000.

5. **Results:** Post-processing the CFD simulation results to obtain useful analytical data.

5. Results and Discussion

5.1. Drag and Lift Coefficients for 0° Angle of Attack

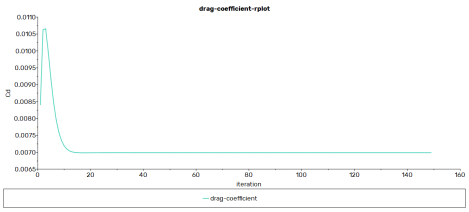

Figure 2. *Drag Coefficient for AOA=0°*

We get the steady state value for the drag coefficient to be 0.07.

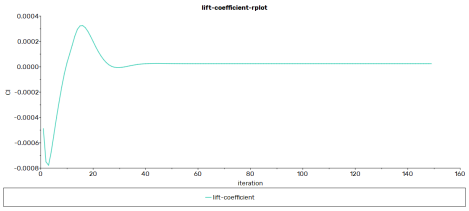

Figure 3. *Lift Coefficient for AOA=0°*

We get the steady state value for the coefficient of lift to be 0.

5.2. Drag and Lift Coefficients for 5° Angle of Attack

For obtaining the drag and lift coefficients for AOA=5°, instead of rotating the airfoil in the simulation, we consider the airfoil to remain horizontal and the flow to be at an angle of 5° to it.

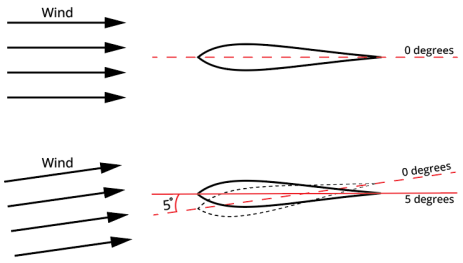

Figure 4. *Enter Caption*

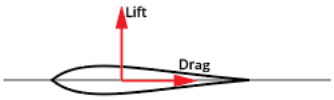

Figure 5. *Direction of Lift and Drag on an Airfoil*

We know that the freestream velocity $U_\infty = 30$ m/s, and the AOA=5°

$$u = U_\infty \cos AOA$$

$$\therefore u = 29.8858 \text{ m/s}$$

$$v = U_\infty \sin AOA$$

$$\therefore v = 2.6147 \text{ m/s}$$

We must also calculate the new force vectors for the drag and the lift. Lift is always perpendicular to the plane of the airfoil, and drag is perpendicular to the lift and in the plane of the airfoil.

$$\hat{x}_l = \sin AOA = 0.0871$$

$$\hat{y}_l = \cos AOA = 0.9962$$

$$\hat{x}_d = \cos AOA = 0.9962$$

$$\hat{y}_d = \sin AOA = 0.0871$$

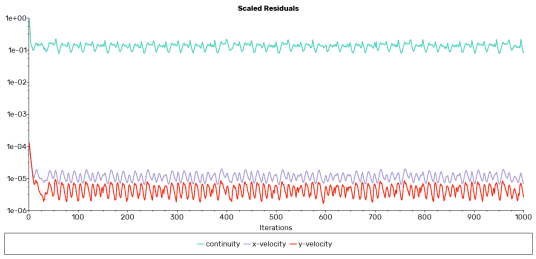

Figure 6. *Scaled Residuals for AOA=5°*

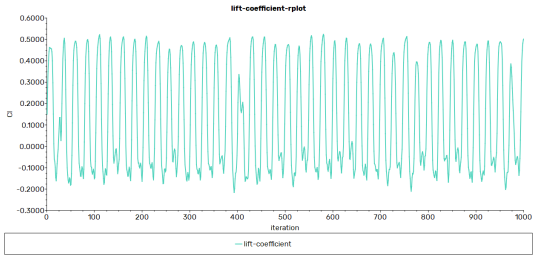

Figure 7. *Lift Coefficient for AOA=5°*

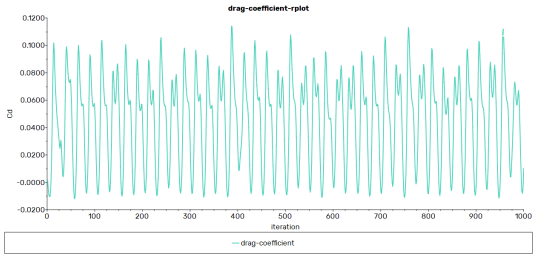

Figure 8. *Drag Coefficient for AOA=5°*

5.3. Comparison of CFD Results for c_d and c_l with Literature

[3]

AOA	Parameter	CFD Results (from ANSYS)	Literature
0°	c_d	0.007	Between 0.005 and 0.009
0°	c_l	0	0
5°	c_d	Between 0.1139 and -0.0120	Between 0.006 and 0.009
5°	c_l	Between 0.5022 and -0.2160	0.5

Table 4. *Comparison of CFD Results with Literature*

5.4. Velocity, Pressure and Streamline Contours

AOA=0°

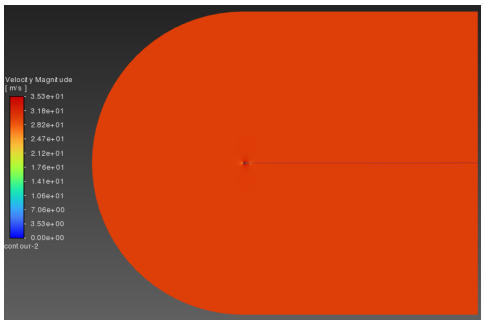

Figure 9. *Velocity Contours for AOA=0°*

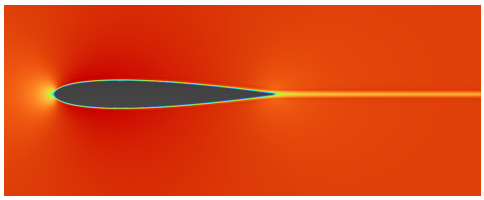

Figure 10. *Velocity Contours (zoomed in)*

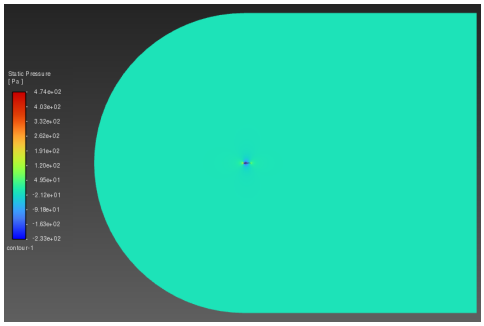

Figure 11. *Pressure Contours for AOA=0°*

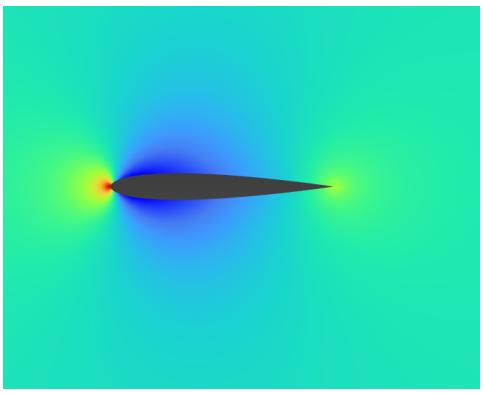

Figure 12. *Pressure Contours (zoomed in)*

AOA=5°

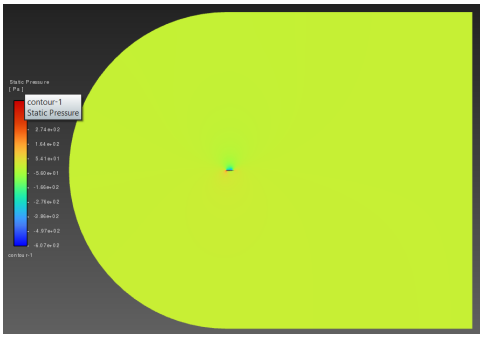

Figure 13. *Pressure Contours for AOA=5°*

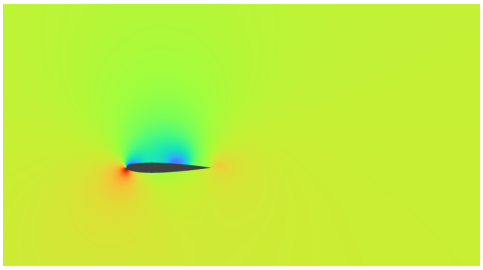

Figure 14. *Pressure Contours (zoomed in)*

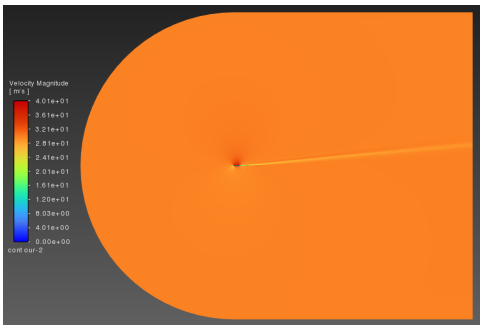

Figure 15. *Velocity Contours for AOA=5°*

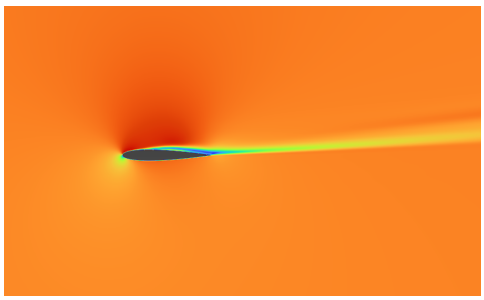

Figure 16. *Velocity Contours (zoomed in)*

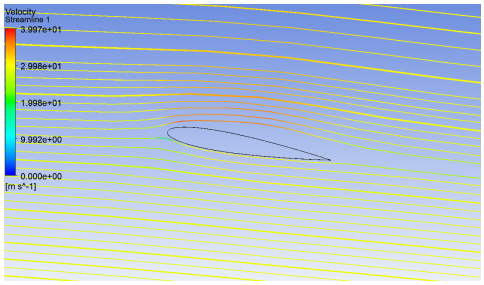

Figure 17. *Streamline Contours for AOA=5°*

5.5. Flow Features in the Contours

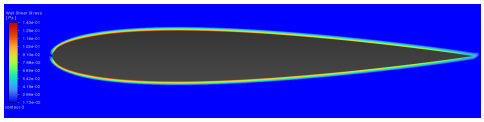

Figure 18. *Wall Shear Stress for AOA=0°*

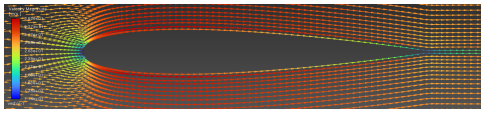

Figure 19. *Velocity Vector Field for AOA=0°*

1. **Boundary Layer Development:**
   - *Velocity Vector Field (Fig. 22)*: Initially, near the pipe's entrance, the velocity profile is relatively uniform, with maximum velocity at the center and decreasing towards the walls due to the no-slip condition. As the fluid moves downstream, the velocity profile develops a parabolic shape. Near the pipe walls, the velocity gradients are higher due to the no-slip condition, and the velocity decreases rapidly. This variation in velocity creates shear stress at the Wall, initiating the boundary layer development.
   - *Strain Rate Contour (Fig. 23)*: The strain rate, which represents the deformation rate within the fluid flow, is highest near the pipe wall, where velocity gradients are the steepest. As fluid particles move along the boundary layer, they experience shear deformation due to the velocity gradient, causing the strain rate to be higher near the Wall.
2. **Boundary Layer Merging:**

- *Velocity Vector Field (Fig. 22)*: In laminar flow, the boundary layer thickness grows gradually along the pipe length due to the continuous accumulation of viscous effects. As the boundary layers from opposite walls grow, they eventually meet at the centerline of the pipe. At this point, the fluid flow in the center of the pipe has a much higher velocity than the fluid near the walls, which leads to a reduced velocity gradient at the centerline.
- *Strain Rate Contour (Fig. 23)*: The strain rate near the centerline of the pipe is lower compared to the near-wall region due to the reduced velocity gradient. This indicates that the deformation rate of the fluid near the centerline is lower.
- *Merging*: When the boundary layers from opposite walls meet at the centerline, the decreasing velocity gradients near the centerline and the lower strain rates indicate a merging of the boundary layers. The flow fully develops at this stage, with a consistent velocity profile across the pipe diameter.

6. Conclusion

This computational fluid dynamics (CFD) study investigated the laminar flow over a NACA 0012 airfoil section using ANSYS software. The analysis aimed to understand the aerodynamic performance, flow behavior, and boundary layer characteristics at angles of attack of 0° and 5°.

The simulation results revealed the formation and development of boundary layers along the airfoil surface. The flow patterns and potential separation regions were identified for both angles of attack through the velocity contours, pressure distributions, and streamlined visualizations.

The drag and lift coefficients were calculated and compared with literature values, providing insights into the aerodynamic forces acting on the airfoil. While the results aligned well with the literature at 0° angle of attack, deviations were observed at 5°, potentially due to limitations in the computational domain or mesh resolution.

The mesh independence study ensured the reliability and accuracy of the simulation results by demonstrating convergence with increasing mesh refinement levels.

Overall, this CFD project contributed to a comprehensive understanding of the laminar flow behavior around the NACA 0012 airfoil, enabling better prediction of aerodynamic forces, flow patterns, and boundary layer characteristics. The insights gained from this analysis can be utilized in optimizing airfoil designs for various applications, such as aircraft wings and turbomachinery blades, ultimately leading to improved aerodynamic performance and efficiency.

References

[1] G. V. “Flow over an airfoil - ansys simulation”. Accessed on 16th April 2024. (2024), [Online]. Available: https://www.youtube.com/watch?v=pspoZ3k7mkY.

[2] Airfoil Tools, *Airfoil Tools - NACA 4-digit*, http://airfoiltools.com/airfoil/naca4digit, Accessed on 16th April 2024.

[3] NASA Turbulence Modeling Resource, *NACA0012 Airfoil Validation Data*, https://turbmodels.larc.nasa.gov/naca0012_val.html, Accessed on 16th April 2024.